

Synergistic Inhibition of 5,6-Diamino-1,10-Phenanthroline with Chloride Ion on Mild Steel Corrosion in 5.5 M H₃PO₄ Containing 2% H₂SO₄ Solution

Fang-Fei Shi, Yan Bai, Feng Zeng, Tao Wu, Yu-Chen Gao, Hao-Zhe Xue, Lin Wang*

School of Chemical Science and Technology, Yunnan University, Kunming 650091 Yunnan Province, P.R. China

*E-mail: wanglin@ynu.edu.cn; wanglin2812@163.com (L. Wang)

Received: 28 October 2022 / Accepted: 1 December 2022 / Published: 27 December 2022

The inhibition behaviors of 5,6-diamino-1,10-phenanthroline (DAPTL) and chloride ion on the corrosion of mild steel in 5.5 M H₃PO₄-2% H₂SO₄ solution have been studied by weight loss, potentiodynamic polarization and electrochemical impedance spectroscopy techniques. The results indicate that combination of DAPTL and Cl⁻ shows stronger synergistic inhibition effect on mild steel corrosion in 5.5 M H₃PO₄-2% H₂SO₄ solution. The Electrochemical studies indicate that DAPTL alone or the combination of DAPTL and Cl⁻ acts as a mixed type inhibitor retarding the anodic and cathodic corrosion reactions and does not change the mechanism of either mild steel dissolution or hydrogen evolution reaction. The corrosion reaction is controlled by charge transfer process. The adsorption of the inhibitors on the mild steel surface follows the Langmuir adsorption isotherm model. The thermodynamic and kinetic parameters (K_{ads} , ΔG°_{ads} , ΔH°_{ads} , ΔS°_{ads} , and E_a) have been calculated and discussed. The adsorption of inhibitor molecules on the steel surface is a spontaneous process with physical and chemical adsorption, while chemical adsorption is dominant.

Keywords: Corrosion; mild steel; phosphoric acid; inhibitor; synergism.

1. INTRODUCTION

As a medium strength acid, phosphoric acid is also highly corrosive to steel [1-3]. The corrosion inhibition researches of steel in phosphoric acid are relatively few in general, and these researches are mainly conducted in solutions with lower phosphoric acid concentration [4-15]. There are also a few studies on the corrosion of stainless steel in higher concentration of phosphoric acid [16-21]. The concentration of phosphoric acid produced in industry is relatively high. For example, the phosphoric acid concentration obtained by the dihydrate wet method process is about 4-5.5 M H₃PO₄ (30% ~ 40% H₃PO₄), while 7.5-9 M H₃PO₄ (55% ~ 63% H₃PO₄) can be produced by the hemihydrate wet method

process [22]. Among them, the dihydrate wet-method process is the most widely used in the production of phosphoric acid. Obviously, the corrosion of metal production equipment cannot be neglected in phosphorus chemical production. In fact, phosphoric acid produced by wet-method process is a mixed acid, which contains about 2% sulfuric acid [22]. The result is more corrosion of metal equipment. Physical protection methods are mainly applied in phosphoric acid production. For instance, the protective steel lining rubber and lining tiles have been used to prolong the service life of production equipment, and even a few core parts are made of high-grade stainless steel [22]. After using for a period of time, these protective lining rubber and tiles required to be replaced with new ones. Of course, high-grade stainless steel will also be corroded during use gradually. It is an effective, convenient and economical method to apply corrosion inhibitor to metal corrosion prevention [23-24].

Generally, the inhibition performance of inhibitor depends largely on the existence of functional groups and heteroatoms, their structures and electronic properties, especially at the aromaticity, the donor sites and the properties of π orbital donating electrons [25-28].

During phosphoric acid production, chloride impurities contained in phosphate rock will be brought into the production process and difficult to completely remove. The existence of chloride ions will cause a certain degree of harm to stainless steel [22, 29]. Chloride ion can induce pitting corrosion of stainless steel [30-31]. However, some researches also indicate that chloride ion can also inhibit corrosion of mild steel in acid solution to varying degrees, and it shows better synergistic inhibition effects with other corrosion inhibitors [32-35]. As one of the most important engineering metal materials, mild steel is widely used in many industries as a construction material because of its low cost and excellent mechanical properties [36].

5,6-diamino-1,10-phenanthroline (DAPTL) is a derivative of o-phenanthroline chemical indicator and is often used as an intermediate in drug synthesis, but it is also environmentally friendly. DAPTL contains more nitrogen atoms unshared electron pairs and abundant π -electrons heterocyclic, which could transfer the unshared electron pairs to the *d*-orbitals of iron surface atoms. This nitrogen-containing heterocyclic compound should meet the requirements as an inhibitor for the corrosion of steel in acid solution. At the same time, it can also be considered that the chloride ion, an impurity existing in the production of wet process phosphoric acid, has certain corrosion inhibition. This impurity can be used to play a beneficial role. In this work, aiming at the actual concentration of phosphoric acid and mixed acid medium in the industrial production of dihydrate wet process phosphoric acid, synergistic inhibition of DAPTL and chloride ion on mild steel has been studied in a mixed acid solution of 5.5 M phosphoric acid with the addition of 2% sulfuric acid (5.5 M H_3PO_4 -2% H_2SO_4) by potentiodynamic polarization, electrochemical impedance spectroscopy and weight loss techniques.

2. EXPERIMENTAL METHODS

2.1 Materials

The chemical composition of mild steel for experiment (wt%): 0.15% C, 0.18% Si, 0.038% Mn, 0.016% P, 0.017% S and Fe balance.

The experimental solutions were prepared with bidistilled water and AR grade H₂SO₄, H₃PO₄ and KCl were used too. 5,6-diamino-1,10-phenanthroline (96%) was supplied by Macklin Biochemical Co. Ltd. The chemical structure of DAPTIL is shown in Figure 1.

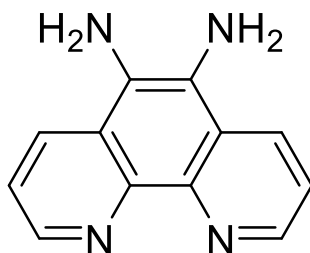


Figure 1. Structure of DAPTIL.

2.2 Gravimetric measurements

The experimental steel sheets (40 mm × 15 mm × 0.4 mm) were carefully polished with emery papers (800 - 2000 grade), then washed with distilled water, degreased with acetone, and dried in air flow.

The steel sheets were immersed into the experimental solutions (150 mL) for 2 hours in air without bubbling after weighing. At the end of the experiments, the sheets were taken out, cleaned with water and acetone, dried and weighed immediately. The testing temperatures of weight loss experiments are 20, 25, 30 and 35°C respectively. Each measurement was performed on three separate samples and the average weight loss was taken.

2.3 Electrochemical measurements

The electrochemical measurements were carried out in a three-electrode cell. The saturated calomel electrode (SCE) was used as the reference electrode and the platinum foil electrode as the auxiliary electrode. The working electrodes (1.0 cm²) were embedded in PVC holder using epoxy resin. The testing surface of working electrode was polished with emery papers from 800 to 2000 grades, then washed with distilled water, degreased with acetone, and dried in air flow. The working electrode needed to be immersed in 250 mL testing solution at open circuit potential (OCP) for 2 hours, and the electrochemical experiment started after the corrosion potential reaches a stable state.

The electrochemical experiments were tested by PARSTAT 2263 Potentiostat/Galvanostat. The potentiodynamic polarization curves were gained by polarizing from -350 mV to + 450 mV with respect to OCP, at a scan rate of 1 mV s⁻¹. The electrochemical impedance spectroscopy (EIS) tests were conducted in the frequency range of 10 mHz to 100 kHz using a 10 mV peak to peak voltage excitation. Each experiment was made in triplicate to assure its reproducibility at 25°C.

3. RESULTS AND DISCUSSION

3.1 Weight loss measurements

The corrosion rate curves of mild steel with different concentrations of DAPTL without and with 30 mM Cl⁻ in 5.5 M H₃PO₄-2% H₂SO₄ are shown in Figure 2 at different temperatures.

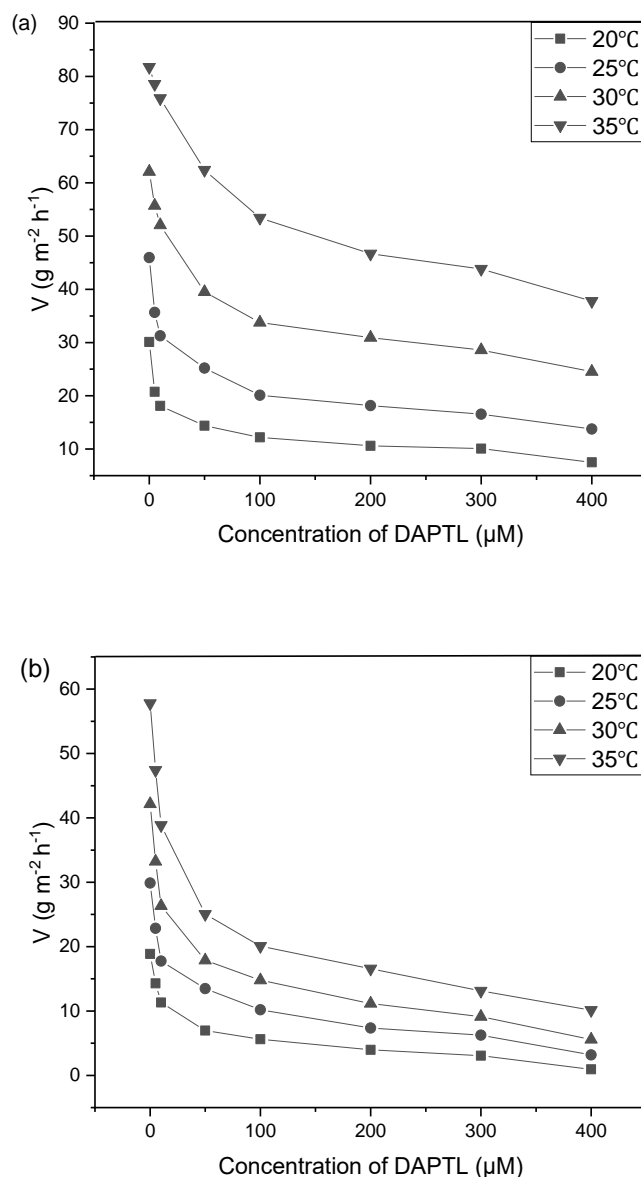


Figure 2. Relationship between corrosion rate and concentration of DAPTL in the absence (a) or presence (b) of Cl⁻ in 5.5 M H₃PO₄-2% H₂SO₄ solution.

It is seen from Figure 2(a), the corrosion rate of the steel decreases gradually as the concentration of DAPTL increases, while the corrosion rate increases with the increase in the temperature. Figure 2(b) gives the relationship of corrosion rate and DAPTL concentration when 30 mM Cl⁻ is added. Compared with Figure 2(a), it is clear that the corrosion rate has been significantly reduced corresponding to the

same DAPTL concentration in the presence of 30 mM Cl⁻ for all the temperature ranges studied and the corrosion rate values are obviously slowed down above 100 mM DAPTL.

The inhibition efficiency (*IE*) is calculated as follows:

$$IE = \frac{V_0 - V_i}{V_0} \times 100 \quad (1)$$

where V_0 and V_i are the weight losses per unit area per unit time in the absence and presence of the inhibitor, respectively.

Inhibition efficiencies obtained by the weight loss method for different concentrations of DAPTL without and with Cl⁻ are given in Table 1.

Table 1. Inhibition efficiencies for different concentrations of DAPTL in 5.5 M H₃PO₄-2% H₂SO₄ solution with and without addition of 30 mM Cl⁻ at different temperatures.

DAPTL (μM)	Cl ⁻ (mM)	Inhibition efficiency			
		20°C	25°C	30°C	35°C
0	0	—	—	—	—
5	0	31.1	22.4	10.2	3.91
10	0	39.8	32.0	16.2	7.17
50	0	52.2	45.2	36.2	23.7
100	0	59.5	56.3	45.6	34.7
200	0	64.8	60.5	50.2	42.9
300	0	66.5	64.1	53.9	45.2
400	0	75.1	70.1	60.5	53.8
0	30	37.3	35.0	32.1	29.3
5	30	52.5	50.3	46.5	42.0
10	30	62.4	61.4	57.6	52.5
50	30	76.9	70.7	71.2	69.4
100	30	81.3	77.8	76.2	75.4
200	30	86.8	84.0	82.0	79.7
300	30	89.8	86.4	85.3	83.9
400	30	96.9	93.1	91.0	87.6

From Table 1, the *IE* increases gradually with increasing DAPTL concentration in the absence of Cl⁻, while the *IE* decreases with experimental temperature increased, which implies the corrosion inhibition of DAPTL for mild steel might be caused by the adsorption of DAPTL on the steel surface. DAPTL may also desorb from the steel surface at higher temperature. Although Cl⁻ (30 mM) alone has certain corrosion inhibition performance, it does not show a good inhibition efficiency.

When the 30 mM Cl⁻ is added into the 5.5 M H₃PO₄-2% H₂SO₄ solutions containing the different concentrations of DAPTL, it is clear that the *IE*s are quite improved compared with the only in the presence of single DAPTL or Cl⁻. For instance, at 400 mM DAPTL, the *IE* of the complex (DAPTL and

Cl⁻) has reached to 96.88% at 20 °C, which means that the combination of DAPTL and Cl⁻ is effective inhibitor for the corrosion of mild steel in 5.5 M H₃PO₄-2% H₂SO₄ solution.

3.2 Adsorption isotherm

It is assumed that the corrosion inhibition is caused by the adsorption of DAPTL, and the surface coverage (θ) is evaluated by weight loss measurement using the method of Sekine [37]:

$$\theta = \frac{V_0 - V}{V_0 - V_m} \quad (2)$$

where V is the corrosion rate with addition of inhibitor and V_m is the smallest corrosion rate.

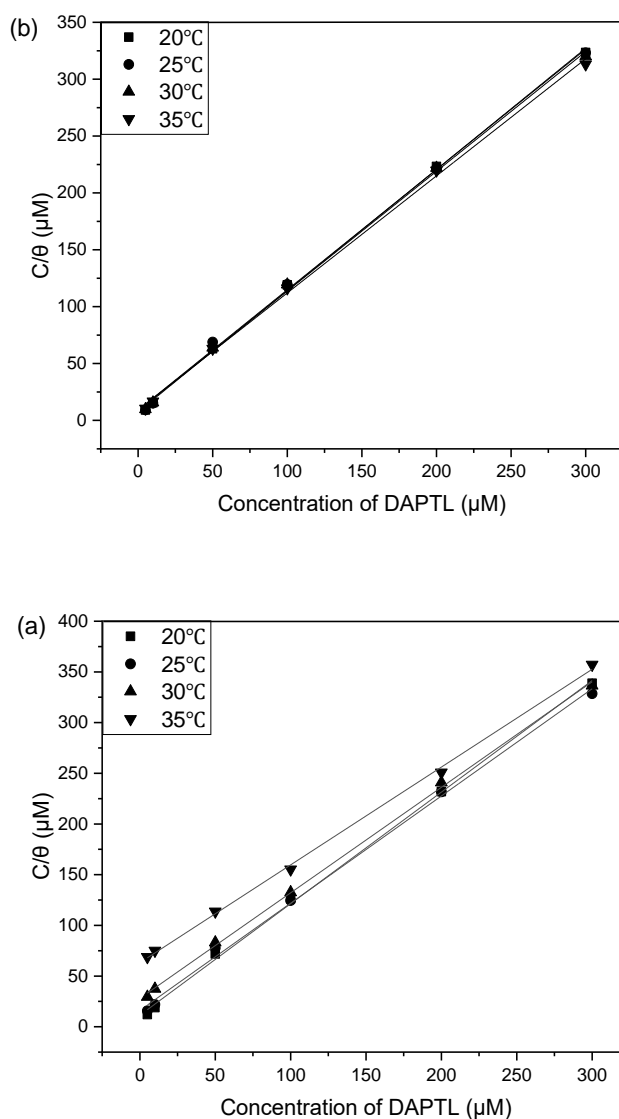


Figure 3. C/θ - C curves for various concentrations of DAPTL in the absence (a) or presence (b) of Cl⁻ in 5.5 M H₃PO₄-2% H₂SO₄ solution.

The results show that the experimental data are in good agreement with Langmuir adsorption isotherm:

$$\frac{C}{\theta} = \frac{1}{K_{ads}} + C \quad (3)$$

where K_{ads} is the adsorptive equilibrium constant and C is the concentration of the inhibitor.

The relationship between C/θ and C are shown in Figure 3 and the corresponding parameters calculated are also given in Table 2.

Table 2. Parameters of the linear regression between C/θ and C .

Inhibitor	Temperature (°C)	Linear regression coefficient	K_{ads} ($\times 10^4 \text{ M}^{-1}$)
DAPTL	20	0.9988	8.81
DAPTL	25	0.9977	6.20
DAPTL	30	0.9992	3.57
DAPTL	35	0.9988	1.58
DAPTL+Cl	20	0.9991	13.3
DAPTL+Cl	25	0.9988	12.1
DAPTL+Cl	30	0.9988	11.7
DAPTL+Cl	35	0.9988	10.9

Obviously, the linear regression coefficient values show that in 5.5 M H_3PO_4 -2% H_2SO_4 solution, the adsorption of the inhibitors on the surface of mild steel conforms to Langmuir adsorption isotherm. From the Table 2, it can also be seen the value of K_{ads} is relatively large and reaches the order of 10^4 or 10^5 , indicating that the adsorption trend of DAPTL on the steel surface is strong. Compared the values of K_{ads} measured in the presence and absence of 30 mM Cl^- , it is found that the values of K_{ads} in the presence of Cl^- are greater than those in the absence of Cl^- , which means that the combination of DAPTL and Cl^- had a larger trend of adsorption on the mild steel surface in 5.5 M H_3PO_4 -2% H_2SO_4 solution.

3.3 Thermodynamic parameters

The thermodynamic model is helpful to explain the adsorption phenomenon of corrosion inhibitor. According to the Van't Hoff equation [38]:

$$\ln K_{ads} = \frac{-\Delta H_{ads}^{\circ}}{RT} + B \quad (4)$$

where ΔH_{ads}° is the standard adsorption heat, T is the absolute temperature, R is the universal gas constant and B is a constant. Clearly, the adsorption heat can be calculated from equation (4) by regression slope.

The standard free energy of adsorption (ΔG_{ads}°) can be obtained by the formula [39-40]:

$$K_{ads} = \frac{1}{55.5} \exp\left(\frac{-\Delta G_{ads}^{\circ}}{RT}\right) \quad (5)$$

where the value 55.5 is the concentration of water in solution expressed in molar. Then the standard adsorption entropy (ΔS_{ads}°) can be gained from the thermodynamic basic equation:

$$\Delta G_{ads}^{\circ} = \Delta H_{ads}^{\circ} - T\Delta S_{ads}^{\circ} \quad (6)$$

All the obtained thermodynamic parameters are listed in Table 3.

Table 3. The thermodynamic parameters for adsorption of DAPTL with and without Cl^- on the mild steel surface at different temperatures in 5.5 M H_3PO_4 -2% H_2SO_4 solution.

Temperature (°C)	Cl^- (mM)	ΔG_{ads}° (kJ mol ⁻¹)	ΔH_{ads}° (kJ mol ⁻¹)	ΔS_{ads}° (J mol ⁻¹ K ⁻¹)
20	0	-38	-85	-160
25	0	-37	-85	-161
30	0	-37	-85	-158
35	0	-35	-85	-162
20	30	-38	-9	99
25	30	-39	-9	101
30	30	-40	-9	102
35	30	-40	-9	101

Generally speaking, values of ΔG_{ads}° is around -20 kJ mol⁻¹ or lower, which is consistent with the electrostatic interaction (physical adsorption) between charged molecules and charged metals, while those more negative than -40 kJ mol⁻¹ are related to chemical adsorption which implies charge sharing or transferring from the inhibitor molecules to the metal surface to form a coordinate bond [41-42]. The calculated ΔG_{ads}° values are close to -40 kJ mol⁻¹ in the absence or presence of Cl^- , which implies that the adsorption mechanism of the DAPTL on the steel surface in 5.5 M H_3PO_4 -2% H_2SO_4 solution is spontaneous and involves mixed adsorption of physical and chemical adsorption, but chemical adsorption is absolutely dominant. The physical adsorption could occur between the active positive centers on the metal surface and π -bonds in the benzene ring of DAPTL or Cl^- , and it can also occur between the negatively charged position of the metal surface and the protonated amino group in DAPTL, while the chemical adsorption is the formation of coordinated bond between the inhibitor molecules and the d-orbital of iron on steel surface through π -electrons or lone pair of electron of N atoms of DAPTL [43-44].

The negative values of ΔH_{ads}° indicates that the adsorption of the inhibitors on the steel surface is an exothermic process. The increase of temperature is unfavorable to the adsorption of inhibitor molecules on the steel surface, which can be reflected by the decrease of inhibition efficiencies with the increase of temperature. In the absence of Cl^- , the negative values of ΔS_{ads}° illustrate that the adsorption is a process accompanied by a decrease of chaos and the exothermic is the principal determinant of spontaneous adsorption of DAPTL on the steel surface. When Cl^- exists, the increase of entropy and

exothermic heat are the driving forces for the spontaneous adsorption reaction of the inhibitor molecules on the steel surface.

3.4 Kinetic parameters

The kinetic model can further clarify the mechanism of the inhibitors.

According to Arrhenius Equation:

$$\ln V = \frac{-E_a}{RT} + \ln A \quad (7)$$

where A is pre-exponential factor and E_a is apparent activation energy. The Arrhenius plots of $\ln V$ vs. $1/T$ are given in Figure 4.

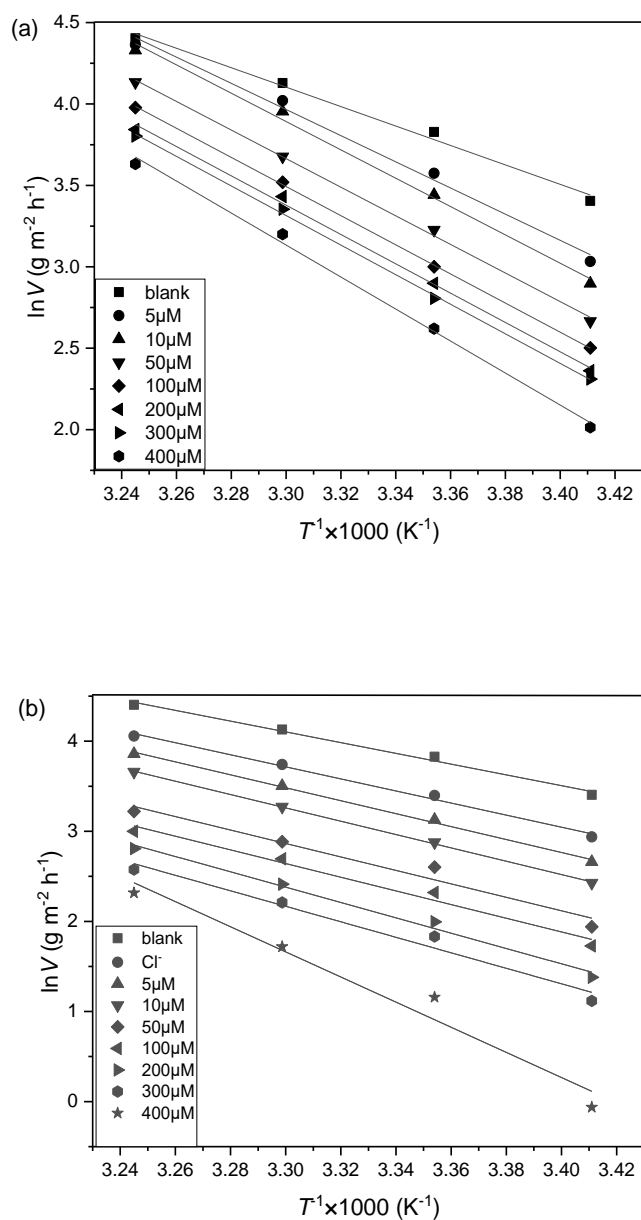


Figure 4. The relationship between $\ln V$ and $1/T$ in the absence (a) or presence (b) of Cl^- .

Table 4. Parameters of the linear regression between $\ln V$ and $1/T$.

DAPTL (μM)	Cl^- (mM)	E_a (kJ mol^{-1})	Pre-exponential factor A ($\text{g m}^{-2} \text{h}^{-1}$)	Linear regression coefficient
0	0	50	2.16×10^{10}	0.9916
5	0	67	1.72×10^{13}	0.9926
10	0	72	1.44×10^{14}	0.9952
50	0	73	1.49×10^{14}	0.9982
100	0	74	2.16×10^{14}	0.9997
200	0	75	2.34×10^{14}	0.9976
300	0	76	2.83×10^{14}	0.9990
400	0	82	2.76×10^{15}	0.9961
0	30	56	1.64×10^{11}	0.9941
5	30	60	6.42×10^{11}	0.9950
10	30	61	1.05×10^{12}	0.9994
50	30	62	1.09×10^{12}	0.9641
100	30	63	1.16×10^{12}	0.9794
200	30	71	1.68×10^{13}	0.9904
300	30	72	1.85×10^{13}	0.9734
400	30	116	5.05×10^{20}	0.9650

E_a and A calculated by liner regression between $\ln V$ and $1/T$ at different concentrations of DAPTL are given in Table 4.

It has been reported that the higher E_a value in the presence of corrosion inhibitor compared with the blank solution is considered to be physical adsorption through the formation of an electrostatic adsorption film on the steel surface in the first stage [45-46]. Since electrochemical corrosion is related to heterogeneous reaction, the pre-exponential factor A is relevant to the number of active centers. There are two possibilities for the active centers with different E_a on the steel surface: (1) The activation energy is higher in the presence than absence of the inhibitor, indicating that the inhibitor is adsorbed on most active adsorption sites (having lowest energy) and the corrosion mainly occurs at the active sites (having higher energy); (2) The activation energy in the presence of the inhibitor is lower than that of the blank solution, which indicates that a smaller number of more active sites are still uncovered during the corrosion process.

The apparent activation energy acts as a function of concentration of DAPTL by the Table 4. The E_a values in the presence of single DAPTL or DAPTL+ Cl^- are higher than those in the uninhibited acid solution and increase with the increase of DAPTL concentration. Therefore, it is obvious that the adsorption of DAPTL or DAPTL+ Cl^- on the steel surface blocks the active sites in the acidic solution, thereby increasing the apparent activation energy. From the equation 7, it can be seen that the corrosion rate of steel is determined by E_a and A at a certain temperature. However, it is also obvious that E_a has

greater influence on steel corrosion than A, which indicates that E_a is the main determinant of reducing steel corrosion rate by increasing the concentration of corrosion inhibitor.

3.5 Polarization measurements

Figure 5 respectively shows the potentiodynamic polarization curves of mild steel for different concentrations of DAPTL in the absence (a) and presence (b) of 30 mM Cl^- in 5.5 M H_3PO_4 -2% H_2SO_4 solution at 25 °C.

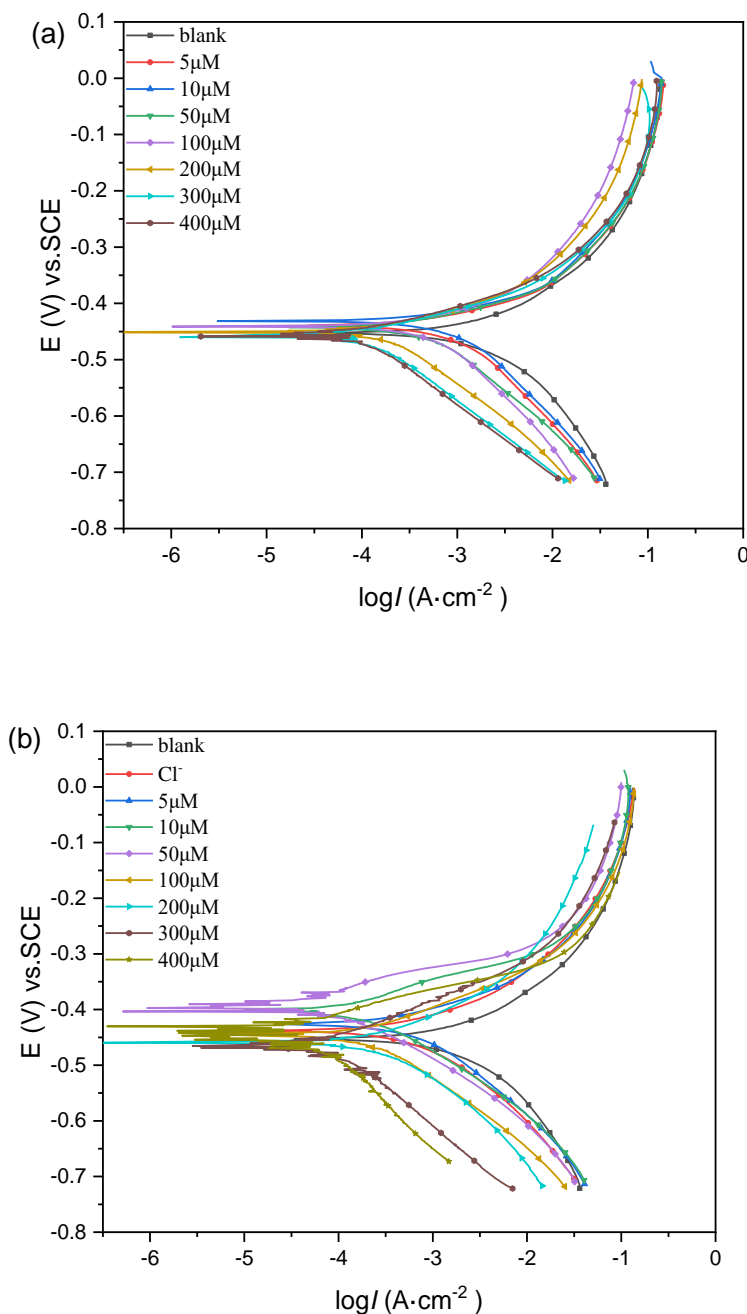


Figure 5. Polarization curves for various concentrations of DAPTL in the absence (a) or presence (b) of Cl^- in 5.5 M H_3PO_4 -2% H_2SO_4 solution at 25 °C.

It can be seen from Figure 5(a) that the presence of a single DAPTL makes the corrosion potential slightly move to the negative and positive direction and caused a decrease of current density of cathode or anode, while the cathode branch obviously moves to the negative potential direction, indicating that the retardation of cathode reaction is dominant. The results imply that DAPTL acts as a mixed type inhibitor that mainly inhibits cathodic reaction for mild steel corrosion in 5.5 M H₃PO₄-2% H₂SO₄ solution. Figure 5(a) compared with figure 5(b), with the addition of 30 mM Cl⁻, it is obvious that the shifting levels of cathodic and anodic with Cl⁻ is much greater than those without Cl⁻, and the combination of DAPTL and Cl⁻ only changes corrosion potential in the negative and positive directions to a certain extent. These results mean that the combination of DAPTL and Cl⁻ acts as a mixed type inhibitor too for mild steel corrosion in 5.5 M H₃PO₄-2% H₂SO₄ solution.

The inhibition efficiency (IE_i) can be calculated by the following formula:

$$IE_i = \frac{I_{corr}^0 - I_{corr}^{inh}}{I_{corr}^0} \times 100 \quad (8)$$

where I_{corr}^0 and I_{corr}^{inh} are the corrosion current density values in the absence and presence of inhibitors, respectively.

The electrochemical polarization parameters for the mild steel corrosion in 5.5 M H₃PO₄-2% H₂SO₄ solution were calculated by Tafel plots and listed in Table 5.

Table 5. Electrochemical parameters and inhibition efficiencies for mild steel in 5.5 M H₃PO₄-2% H₂SO₄ solution at 25 °C.

DAPTL (μM)	Cl ⁻ (mM)	$-E_{corr}$ (vs. SCE) (mV)	I_{corr} (μA cm ⁻²)	$-\beta_c$ (mV dec ⁻¹)	β_a (mV dec ⁻¹)	IE_i
0	0	452	329	37	30	—
5	0	439	207	38	30	37.1
10	0	431	190	35	26	42.2
50	0	443	172	47	34	47.7
100	0	439	129	38	26	60.8
200	0	451	98.6	48	39	70.0
300	0	453	66.2	60	38	79.9
400	0	448	52.8	47	35	84.0
0	30	441	230	70	52	30.1
5	30	426	198	66	40	39.8
10	30	404	163	84	41	50.5
50	30	395	121	77	56	63.2
100	30	442	90.0	70	38	72.6
200	30	459	59.0	63	42	82.1
300	30	461	35.0	89	54	89.4
400	30	443	8.30	56	45	97.5

As can be seen from the Table 5, the values of β_a and β_c do not show significantly changes and there is no regular change in the slopes of the Tafel lines with the change of the inhibitor concentrations,

which illustrates that the corrosion reaction mechanisms of anodic steel dissolution and cathodic hydrogen evolution have not been changed [47]. It appears that inhibition occurred by a blocking mechanism on the available metal active centers [48]. Comparing the values of the I_{corr} and IE_i without and with Cl^- , it can be seen that in the presence of Cl^- the corrosion current density decreases and the corrosion inhibition efficiency increases effectively, which also shows that the combination of DAPTL and Cl^- is an effective inhibitor for mild steel in 5.5 M H_3PO_4 -2% H_2SO_4 solution.

3.6 Electrochemical impedance spectroscopy

Nyquist plots of mild steel in 5.5 M H_3PO_4 -2% H_2SO_4 solution for DAPTL as inhibitor without (a) and with (b) 30 mM Cl^- are given in Figure 6 at 25 °C, respectively.

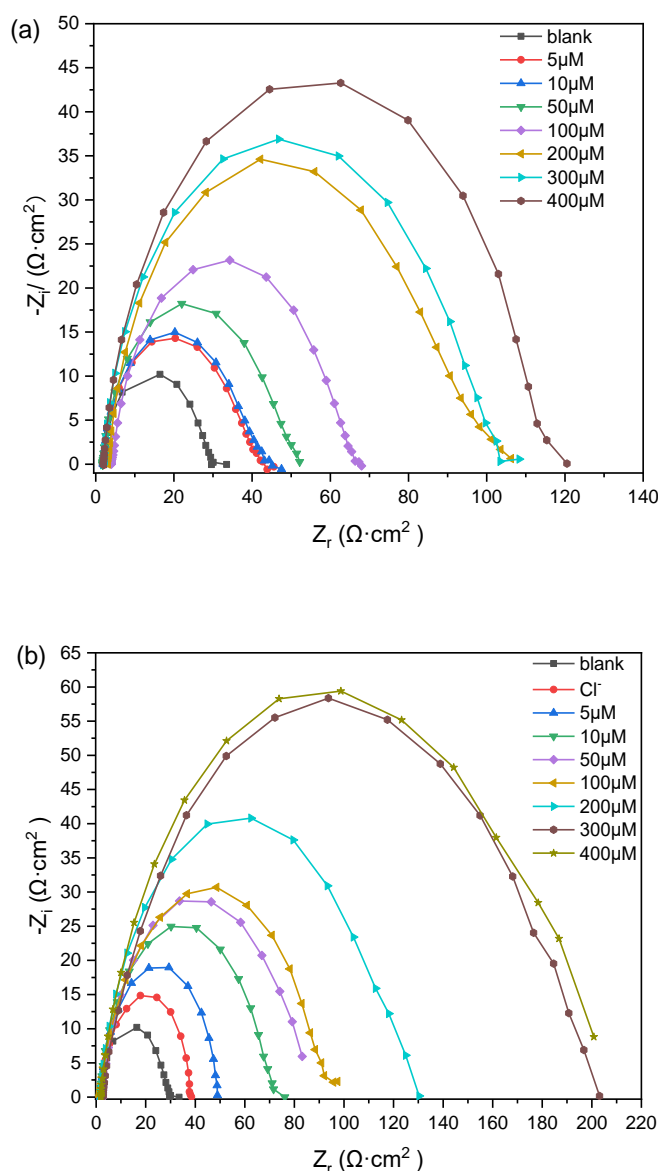


Figure 6. EIS for various concentrations of DAPTL in the absence (a) or presence (b) of Cl^- in 5.5 M H_3PO_4 -2% H_2SO_4 at 25 °C.

All electrochemical impedance spectra are shown as a single depressed capacitive loop in the presence or absence of the inhibitors for mild steel in 5.5 M H₃PO₄-2% H₂SO₄ solution, indicating that the charge-transfer process mainly affects the corrosion inhibition of steel and the existence of inhibitors does not change the mechanism of steel dissolution [49]. The capacitance loops are not perfect semicircle due to the frequency dispersion caused by the roughness and inhomogeneous of the electrode surface [49-50]. The semicircle diameters increase with the increasing DAPTL concentration. However, it can also be clearly seen that the diameters of the capacitance loops containing Cl⁻ are larger than those without Cl⁻, which means that the protection barrier become more thickly packed over the surface of steel and Cl⁻ can effectively promote the corrosion anti-corrosion performance of DAPTL.

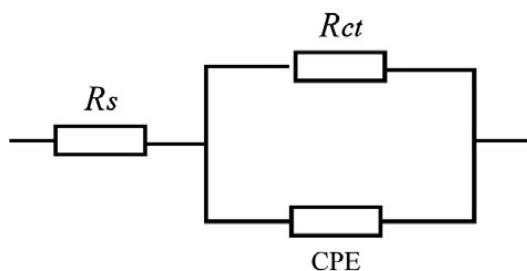


Figure 7. Equivalent circuit model used to fit the EIS experiment data.

The EIS results are analyzed according to the equivalent circuit model, shown in Figure 7, which includes constant phase element (CPE), solution resistance (R_s) and charge transfer resistance (R_{ct}). The double layer capacitance (C_{dl}) value affected by imperfections of the surface is simulated via CPE [51].

Table 6. Impedance parameters and inhibition efficiencies for mild steel in 5.5 M H₃PO₄-2% H₂SO₄ solution at 25 °C.

DAPTL (μ M)	Cl ⁻ (mM)	R_s (Ω cm ²)	C_{dl} (μ F cm ⁻²)	R_{ct} (Ω cm ²)	IE_{ct}
0	0	2.05	229	26.8	
5	0	1.86	198	38.9	31.1
10	0	1.90	195	40.1	33.2
50	0	1.87	178	50.5	46.9
100	0	1.82	148	61.1	56.1
200	0	1.82	120	93.5	71.3
300	0	1.82	115	101	73.5
400	0	1.95	87.0	115	76.7
0	30	1.84	204	36.7	27.0
5	30	1.82	185	47.4	43.5
10	30	1.65	127	70.2	61.8
50	30	1.59	123	80.0	66.5
100	30	1.58	105	89.7	70.1
200	30	1.56	98.0	120	77.7
300	30	1.74	72.0	187	85.7
400	30	2.53	68.0	194	86.2

The CPE is composed of a coefficient α and a component Q_{dl} which quantifies different physical phenomena like inhibitor adsorption, porous layer formation, surface inhomogeneous resulting from surface roughness, etc. The C_{dl} is deduced as follows [52]:

$$C_{dl} = Q_{dl} \cdot (2\pi f_{max})^{\alpha-1} \quad (9)$$

where f_{max} represents the frequency at which the imaginary value reaches a maximum on the Nyquist plot. If α is equal to 1, the electrode surface is homogeneous and plane, which can be regarded as an ideal capacitance. Parametrical adjustment of the circuit with experimental impedance spectra gives access to the charge transfer resistance and double layer capacitance. The inhibition efficiencies (IE_{ct}) from EIS were calculated by the equation:

$$IE_{ct} = \frac{R_{ct}^{inh} - R_{ct}^0}{R_{ct}^{inh}} \times 100 \quad (10)$$

Where R_{ct}^{inh} and R_{ct}^0 are the charge-transfer resistances with and without the inhibitor, respectively. The values of EIS parameters are listed in Table 6.

It can be seen from Table 6 that the C_{dl} values decrease in the presence of inhibitor compare to the absence of inhibitor, which means that the adsorption of inhibitor on the mild steel surface forms an adhesion film and increases the thickness of the electric double layer, which may be the reason for the decrease of C_{dl} [53]. It can also be observed that the values of R_{ct} or IE_{ct} increase with the increase of DAPTL concentration, whether Cl^- is present or not. Of course, it is also obvious that the values of R_{ct} or IE_{ct} in the presence of Cl^- are greater than those in the absence of Cl^- . These results are in good agreement with those gained by weight loss and polarization methods.

3.7 Synergistic effect

According to the above researches, the inhibition efficiencies increase more greatly in the presence of DAPTL and Cl^- than those in the presence of single DAPTL, suggesting that there may be a synergistic inhibition effect between DAPTL and Cl^- for mild steel corrosion in 5.5 M H_3PO_4 -2% H_2SO_4 solution. The ion pair interaction between organic cations and chlorine anions may lead to effect of synergistic inhibition to increase the surface coverage which can be explained by synergism parameters (S), described as follow [54-55]:

$$S = \frac{1 - IE_1 - IE_2 + IE_1 \times IE_2}{1 - IE_{1+2}} \quad (11)$$

where IE_1 and IE_2 are the inhibition efficiency for inhibitor 1 and 2, respectively. IE_{1+2} is the inhibition efficiency corresponding to the coexistence of inhibitor 1 and 2.

Generally, when value of S is < 1 , meaning that antagonistic behavior leading to competitive adsorption prevails, whereas $S > 1$ implies a synergistic effect. Table 7 shows the values of S . It can be seen that the S values at all inhibitor concentrations are greater than 1 except that the S value is less than 1 at one concentration, indicating that DAPTL and Cl^- have stronger synergistic inhibition effect on mild steel corrosion and promote the inhibition efficiency to be better improved in 5.5 M H_3PO_4 -2% H_2SO_4 solution.

Table 7. Synergism parameters of DAPTL and Cl⁻ for mild steel corrosion inhibition in 5.5 M H₃PO₄-2% H₂SO₄ solution.

DAPTL (μM)	Cl ⁻ (mM)	Synergism parameters(S)			
		20°C	25°C	30°C	35°C
5	30	0.91	1.02	1.14	1.17
10	30	1.00	1.14	1.34	1.38
50	30	1.30	1.21	1.50	1.76
100	30	1.36	1.28	1.55	1.88
200	30	1.67	1.60	1.88	1.99
300	30	2.08	1.72	2.13	2.41
400	30	5.00	2.80	2.98	2.63

DAPTL is a compound containing amino groups and N heterocycles, which contains lone-pair electrons and π -electrons. It would be protonated in the acid solution as following:



In acid medium, steel surface contains positive charge due to $E_{\text{corr}} - E_q = 0$ (zero charge potential) > 0 [56]. The negatively charged chloride ions would adhere to the positively charged steel surface. However, it is more difficult for the positively charged DAPTL to directly adhere to the positively charged steel surface because of electrostatic repulsion, which also explains the reason that the corrosion inhibition of single DAPTL on mild steel is limited in 5.5 M H₃PO₄-2% H₂SO₄ solution. The zero charge potential becomes less negative since Cl⁻ is easily adsorbed to the positive charge position on the steel surface under the action of electrostatic force, which is favorable for the adsorption of inhibitors in cationic form [57]. The protonated DAPTL can be adsorbed to the negatively charged position on the steel surface. It becomes easier for $[\text{DAPTLH}_x]^{x+}$ to reach the steel surface due to the electrostatic interaction between $[\text{DAPTLH}_x]^{x+}$ and Cl⁻. The adsorption of DAPTL could occur through donor-acceptor interactions between the abundance π -electrons or nitrogen atoms of DAPTL and the vacant d-orbital of surface iron atoms. Thus, both physical and chemical adsorption can work on the steel surface. It can be said that Cl⁻ acts as a bridge.

4. CONCLUSION

(1) DAPTL shows a certain degree of retardation to corrosion of mild steel in 5.5 M H₃PO₄-2% H₂SO₄ solution and the corrosion inhibition increases with the increase of DAPTL concentration. However, with the addition of Cl⁻, the corrosion inhibition is significantly enhanced. The synergism parameters reveal that DAPTL and Cl⁻ display strong synergistic inhibition effect for mild steel corrosion in 5.5 M H₃PO₄-2% H₂SO₄ solution.

(2) The adsorption of DAPTL on the steel surface follows the Langmuir adsorption isotherm in the presence or absence of Cl⁻. The adsorption of inhibitor molecules on the steel surface is a spontaneous process with physical and chemical adsorption, while chemical adsorption is dominant.

(3) Potentiodynamic polarization results show that DAPTL alone or combination of DAPTL and Cl^- retards the cathodic and anodic reaction for mild steel corrosion in 5.5 M H_3PO_4 -2% H_2SO_4 solution, however the cathodic polarization is dominant for the presence of single DAPTL. DAPTL alone or combination of DAPTL and Cl^- acts as a mixed type inhibitor retarding the anodic steel dissolution and cathodic hydrogen evolution reaction

(4) EIS shows that the fact the corrosion reaction is controlled by charge transfer. The inhibition performances obtained from weight loss, polarization and EIS measurements represent the same trend.

ACKNOWLEDGEMENT

This study was financially supported by the National Innovation and Entrepreneurship of College Students Foundation of Chin (Grant No.202210673095)

References

1. P. B. Mayhure and T. Vasudevan, *Corrosion*, 38 (1982) 171.
2. R. Sánchez-Tovar, M. T. Montañés and J. García-Antón, *Corros. Sci.*, 52 (2010) 1508.
3. H. Iken, R. Basseguy, A. Guenbour and A. B. Bachir, *Electrochim. Acta*, 52 (2007) 2580.
4. T. Sathiyapriya, D. Manikandan, R. Jagadeeswari, R. Govindasamy, S. U. Mohammed Riyaz, K. Moonis Ali and S. Mika, *Mater. Corros.*, 73 (2022) 259.
5. B. Lin, S. Zheng, J. Liu and Y. Xu, *Int. J. Electrochem. Sci.*, 15 (2020) 2335.
6. Y. J. Yang, Y. K. Li, L. Wang, H. Liu, D. M. Lu and L. Peng, *Int. J. Electrochem. Sci.*, 14 (2019) 3375.
7. Y. J. Yang, H. Liu, D.M. Lu, L. Peng and L. Wang, *Int. J. Electrochem. Sci.*, 14 (2019) 5008.
8. X. Li, S. Deng, X. Xie and G. Du, *Mater. Chem. Phys.*, 181 (2016) 33.
9. R. Najjar, A. M. Abdel-Gaber and R. Awad, *Int. J. Electrochem. Sci.*, 13 (2018) 8723.
10. H. Liu, Y.-Ju Yang, L. Wang, S.M. Ma, X.Y. Peng, D.M. Lu, T. Zhao and Z. Wang, *Int. J. Electrochem. Sci.*, 13 (2018) 10718.
11. X. Li, S. Deng, H. Fu and X. Xie, *Corros. Sci.*, 78 (2014) 29.
12. M. Benabdellah, R. Touzani, A. Dafali, B.Hammouti, S and El Kadiri, *Mater. Lett.*, 61 (2007) 1197.
13. L. Tang, X. Li, G. Mu, L. Li and G. Liu, *Appl. Surf. Sci.*, 253 (2006) 2367.
14. T. Poornima, J. Nayak and A.N. Shetty, *Corros. Sci.*, 53 (2001) 3688.
15. L. Wang, *Corros. Sci.*, 48 (2006) 608.
16. A. Mazkour1, S. El Hajjaji1, N. Labjar, El M. Lotfi and M. El Mahi, *Int. J. Electrochem. Sci.*, 16 (2021) 1.
17. M. Ben Salah, R. Sabot, Ph. Refait, I. Liascukiene, C. Méthivier, J. Landoulsi, L. Dhouibi and M. Jeannin, *Corros. Sci.*, 99 (2015) 320.
18. M. Ben Salah, R. Sabot, E. Triki, L. Dhouibi, Ph. Refait and M. Jeannin, *Corros. Sci.*, 86 (2014) 61.
19. C. Escrivà-Cerdán, E. Blasco-Tamarit, D. M. García-García, J. García-Antóna and A. Guenbour, *Electrochim. Acta*, 80 (2012) 248.
20. R. Sanchea-Tovar, M. T. Montanes, J. García- Antóna, A. Guenbour and A. Ben-Bachir, *Corros. Sci.*, 53 (2011) 1237.
21. H. Iken, R. Basseguy and A. A. Ben-Bachir, *Electrochim. Acta*, 52 (2007) 2580.
22. Y. X. Zhang, *Linfei Ji Fuhe Feiliao Gongyixue*, Chemical Industry Press, (2008) Beijing, China.
23. A. Winkler, *Metals*, 7 (2017) 553.
24. S. M. R. Shoia, M. Abdouss and A. A. M. Beiji, *Mater. Corros.*, 3 (2021) 623.
25. M. M. Saleh, M. G. Mahmouda and H. M. Abd El-Lateef, *Corros. Sci.*, 154 (2019) 70.

26. G Sigircik, D. Yildirim and T. Tüken, *Corros. Sci.*, 120 (2017) 184.
27. G. Žerjav, A. Lanzutti, F. Andreatta, L. Fedrizzi and I. Milošev, *Mater. Corros.*, 68 (2017) 30.
28. M. Mobin, R. Aslam and J. Aslam, *Mater. Chem. Phys.*, 191 (2017) 151.
29. A. Pardo, E. Otero, M. C. Merino, M. D. Lopez, M. V. Utrilla and F. Moreno, *Corrosion*, 56 (2000) 411.
30. M. Talebian, K. Raeissi, M. Atapour, B. M. Fernández-Pérez, A. Betancor- Abreu, I. Llorente, S. Fajardo, Z. Salarvand, S. Meghdadi, M. Amirnasr and R. M. Souto, *Corros. Sci.*, 160 (2019) 108130.
31. A. Pardo, E. Otero, M. C. Merino, M. D. Lopez, M. V. Utrilla and F. Moreno, *Mater. Corros.*, 51 (2000) 850.
32. A. Khamis, M. M Saleh and M. I. Awad, *Corros. Sci.*, 66 (2013) 343.
33. J. T. Gong, Y. J. Liu, L. Wang, Y. Q., Y.I. Bai and D. M. Lu, *Int. J. Electrochem. Sci.*, 15 (2020) 4915.
34. S. A. Umoren, O. Ogbobe, I. O. Igwe and E. E. Ebenso, *Corros. Sci.*, 50 (2008) 1998.
35. X. Li, L. Tang, L. Li, G. Mu and G. Liu, *Corros. Sci.*, 48 (2006) 308.
36. N. S. Ayati, S. Khandandel, M. Momeni, M. H. Moayed, A. Davoodi and M. Rahimizadeh, *Mater. Chem. Phys.*, 126 (2011) 873.
37. I. Sekine and Y. Hirakawa, *Corrosion*, 42 (1986) 272.
38. L. Wang, S.W. Zhang, Q. Guo, H. Zheng, D.M. Lu, L. Peng and J. Xion, *Mater. Corros.*, 66 (2015) 594.
39. S. K. Shukla and M. A. Quraishi, *Corros. Sci.*, 51 (2009) 1007.
40. E. Khamis, *Corrosion*, 46 (1990) 476.
41. A. K. Singh and M. A. Quraishi, *Corros. Sci.*, 52 (2010) 1378.
42. E. Machnikova, K. H. Whitmire and N. Hackerman, *Electrochim. Acta*, 53 (2008) 6024.
43. M. A. Hegazy and M. F. Zaky, *Corros. Sci.*, 52 (2010) 1333.
44. J. Flis and T. Zakroczymski, *J. Electrochem. Soc.*, 143 (1996) 2458.
45. E. A. Noor and A. H. Al-Moubaraki, *Mater. Chem. Phys.*, 110 (2008) 145.
46. A. Popova, E. Sokolova, S. Raicheva and M. Christov, *Corros. Sci.*, 45 (2003) 33.
47. A. A. Farag and M. A. Hegazy, *Corros. Sci.*, 74 (2013) 168.
48. K. C. Emergül and M. Hayvalı, *Corros. Sci.*, 48 (2006) 797.
49. L. Larabi, Y. Harek, M. Traisnel and A. Mansri, *J. Appl. Electrochem.*, 34 (2004) 833.
50. N. Labjar, M. Lebrini, F. Bentiss, N. E. Chihib, S. El Hajjaji and C. Jama, *Mater. Chem. Phys.*, 119 (2010) 330.
51. P. Bommersbach, C. Alemany-Dumont, J. P. Millet and B. Normand, *Electrochim. Acta*, 51 (2006) 4011.
52. M. Lagrenée, B. Mernari, M. Bouanis, M. Traisnel and F. Bentiss, *Corros. Sci.*, 44 (2002) 573.
53. M. Behpour, S.M. Ghoreishi, M. Khayatkashani and N. Soltani, *Corros. Sci.*, 53 (2011) 2489.
54. T. Murakawa, S. Nagaura and N. Hackerman, *Corros. Sci.*, 7 (1967) 79.
55. X. Li, S. Deng, X. Xie and G. Du, *Mater. Chem. Phys.*, 181 (2016) 33.
56. A. Döner, E. A. Şuhin, G. Kardaş and O. Serindağ, *Corros. Sci.*, 66 (2013) 278.
57. H. Ashassi-Sorkabi, N. Gahlebsaz-Jeddi, F. Hashemzadeh and H. Jahani, *Electrochim. Acta*, 51 (2006) 3848.